Journal of Solid-Phase Biochemistry, Vol. 3, No. 2, 1978

KINETICS OF IMMOBILIZED HYDROGENASE CATALYSIS

M. S. SAFONOV, G. F. SUD'INA, V. K. BEL'NOV, and S. D. VARFOLOMEEV[1]

Moscow State University
Moscow 117234, U.S.S.R.

Accepted July 31, 1978

Hydrogenase from phototrophic bacteria *Thiocapsa roseopersicina* has been immobilized in polyacrylamide gel membranes. Stability of the preparations thus obtained in the reaction of hydrogen evolution in the system sodium dithionite-methyl viologen-hydrogenase has been studied. Kinetics of immobilized hydrogenase action is discussed. Hydrogen flux values have been determined as functions of sodium dithionite and methyl viologen concentrations and plate thickness. The results obtained are interpreted in terms of a theoretical model of two consecutive heterogeneous reactions. The theory is compared with the experiment; a number of parameters describing enzyme action in membranes are determined from the kinetic data. The kinetic data and the data of other independent experiments have been used to determine the same parameters in order to test model applicability. Good agreement between the theoretical model and the experimental data is observed.

INTRODUCTION

During recent years hydrogen energy converters have been the focus of the ever-increasing interest of researchers due to the unique properties of hydrogen as fuel and as "the universal energy mediator" (1,2). The construction of catalysts for accelerating the formation or consumption of hydrogen is a problem of utmost practical importance. The enzymes of hydrogenase family that effect the activation and formation of molecular hydrogen in biological systems offer promise in this field (3–6). First, studies of the mechanisms of the catalytic action of hydrogenase may prove useful in the construction of corresponding model systems. Second, immobilized enzymes may be used in heterogeneous catalysis.

Soluble and immobilized hydrogenases play important roles as bioenergy converters. Thus a number of water biophotolysis systems producing molecular hydrogen include hydrogenases as terminal enzymes participating in hydrogen formation (7–9). The systems are now known in which

[1]Author to whom correspondence should be addressed. Department of Chemical Enzymology, Moscow State University, Moscow 117234, USSR.

0146-0641/78/0600-0133$05.00/0

hydrogenases catalyze the transfer of electrons to electrodes; these have been utilized in the construction of reversible hydrogen electrodes (10, 11).

Hydrogenases are noted for their lability, rapid thermal inactivation, and oxidation in air. One of the most stable hydrogenases has been isolated from the phototrophic bacteria *Thiocapsa roseopersicina* (12,13). The present work describes immobilization of hydrogenase from *Th. roseopersicina* and the kinetic behavior of the immobilized enzyme.

EXPERIMENTAL

The samples of hydrogenase from *Th. roseopersicina* were kindly provided by I. N. Gogotov of the Institute of Phothosynthesis of the U.S.S.R. Academy of Sciences. The enzyme was isolated as recommended in (13). 4,4'-Dimethyldipyridine chloride (methyl viologen) and sodium dithionite were purchased from Sigma Co. The components of the buffer solutions were of analytical grade.

Hydrogenase from phototrophic bacteria *Th. roseopersicina* was immobilized in a 24% (2% based on *N,N*-methylene bisacrylamide) polyacrylamide gel using a similar procedure to that described in (14). The enzyme and gel were co-polymerized directly in the reaction vessel to produce gel membranes firmly attached to the vessel bottom. Approximately 40% of the enzyme retained its activity on immobilization. Practically no enzyme leakage was observed (wash waters displayed no catalytic activity even after prolonged contact with the gel).

Kinetics of hydrogen formation catalyzed by the hydrogenase were studied with a specially designed thermostated bath reactor which could be filled with an inert gas. Bubbling of an inert gas through the solution and sampling of the gas phase were also possible. The reaction was monitored by measuring the hydrogen concentration in the gas phase on a Chrom-4 gas chromatograph calibrated against standard samples of known concentrations of hydrogen.

Polyacrylamide gel membranes containing immobilized hydrogenase were of various thickness and had a surface area of 10 cm^2. The membranes were kept in stirred buffer solutions at pH 7.8 containing known concentrations of methyl viologen. After saturating a membrane with methyl viologen under anarobic conditions a certain amount of sodium dithionite was introduced into the reaction vessel and the gas phase composition over the solution was analyzed chromatographically. Solution volumes were about 10 times larger than membrane volumes so that the reagent concentrations remained relatively constant during reaction (about 10 h).

RESULTS

Hydrogen evolution from the reduced form of methyl viologen is the "classic" test for hydrogenase activity. The process follows the scheme

$$\begin{gathered}(1/a)S_1 + S_2' \longrightarrow S_2 \\ S_2 + H^+ \xrightarrow{(E)} \tfrac{1}{2}H_2 + S_2'\end{gathered} \qquad (1)$$

where S_1 is sodium dithionite, S_2' and S_2 the oxidized and reduced forms of methyl viologen, respectively, a the number of electrons transferred from the electron donor S_1 to methyl viologen. The first step, that of reduction of methyl viologen with sodium dithionite in solution, is a fast reaction proceeding almost instantaneously. There are experimental proofs of the fact that transformation of methyl viologen into the "blue" reduced form is a one-electron process (15). The second reaction, the enzymatic hydrogen formation, follows Michaelis–Menten kinetics (16). The introduction of sodium dithionite into a solution containing methyl viologen and immobilized enzyme thus induces the formation of molecular hydrogen catalyzed with hydrogenase. After the starting period of about 2 to 3 h, the process developed under steady state conditions characterized by a constant rate of hydrogen evolution. The kinetic patterns were studied under steady state conditions. Since as the reaction rate was independent of the hydrogen partial pressure over the solution, the reverse reaction (that of hydrogen oxidation) was excluded from consideration. The typical kinetic curves are shown in Figure 1. The products of oxidation of sodium dithionite were not

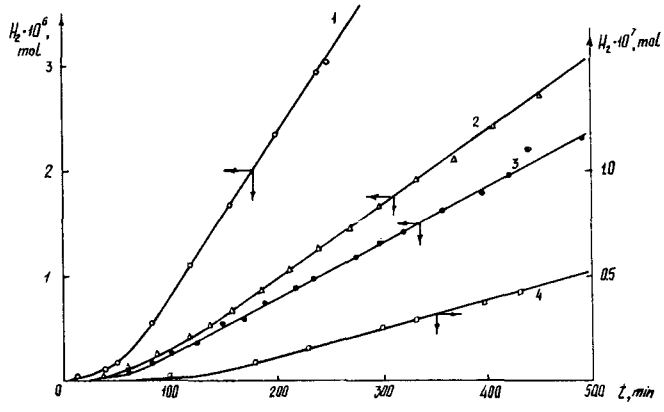

FIG. 1. Kinetic curves of hydrogen evolution in the system immobilized hydrogenase-methyl viologen-sodium dithionite. Membrane thickness is 0.8 cm, surface area is 10 cm^2. Substrate concentrations: (1) $[S_1]_0 = 1.0 \cdot 10^{-2}$M, $[S_2]_0 = 10^{-3}$ M; (2) $[S_1]_0 = 4.2 \cdot 10^{-3}$ M, $[S_2]_0 = 10^{-5}$ M; (3) $[S_1]_0 = 1.4 \cdot 10^{-3}$ M, $[S_2]_0 = 10^{-3}$ M; (4) $[S_1]_0 = 4.2 \cdot 10^{-5}$ M, $[S_2]_0 = 5 \cdot 10^{-7}$ M; pH 7.8, 30°C, 0.1 M phosphate buffer.

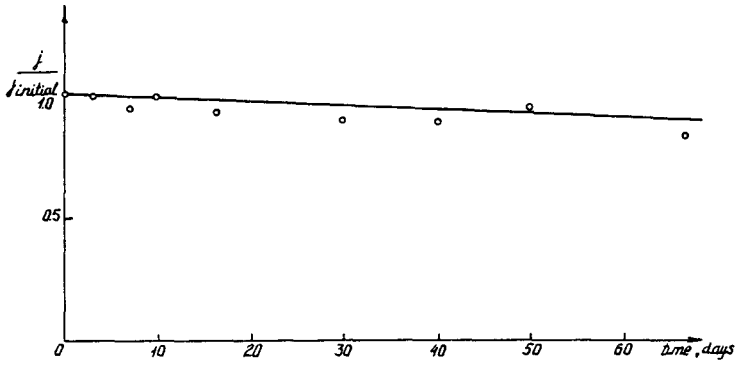

FIG. 2. The experimental stability data on immobilized hydrogenase from *Th. roseopersicina*; pH 7.8, 30°C, 0.1 M phosphate buffer.

identified and the stoichiometric coefficient remained an unknown. According to the data cited in the work (17), methyl viologen may oxidize sodium dithionite to sodium sulphate ($a = 6$); on the other hand, according to (18), a may be 1 or 2 under dithionite excess conditions.

Stability of Immobilized Hydrogenase

We first studied the kinetics of enzyme inactivation. Steady state rates of hydrogen evolution were periodically measured for membranes containing the immobilized enzyme over a period of 2 months. These tests were carried out with relatively thin membranes at saturating concentrations of methyl viologen and sodium dithionite. Under these conditions the rate of hydrogen evolution was independent of both methyl viologen and sodium dithionite concentrations, and variations of enzyme activity with time were determined by its inactivation. The data obtained are given in Figure 2. These data show that hydrogenase from *Th. roseopersicina* when immobilized in polyacrylamide gel membranes has good stability. Enzyme activity remained constant within measurement error over a period of 1 month. This allowed us to study the kinetics of immobilized enzyme action quantitatively.

Steady State Kinetics of Hydrogen Evolution under the Action of Immobilized Hydrogenase Thiocapsa roseopersicina. We have studied hydrogen flows as dependent on the concentrations of the solutes (sodium dithionite, methyl viologen); the concentration of the enzyme in membranes has also been varied. The measurements have been carried out with membranes of 0.1- to 1.0-cm thickness. A series of the experimental data

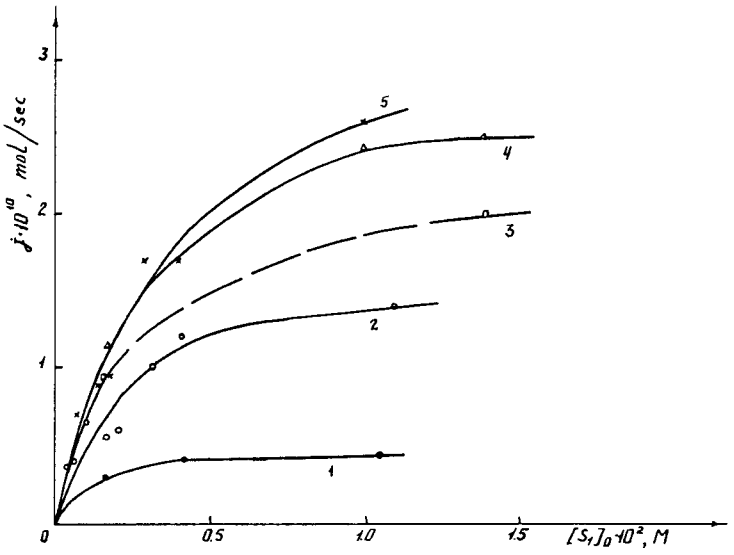

FIG. 3. Hydrogen vs. sodium dithionite experimental curves for various fixed methyl viologen concentrations. Membranes 0.8-cm thick, pH 7.8, 30°C, 0.1 M phosphate buffer. Methyl viologen concentrations: (1) $5 \cdot 10^{-7}$ M, (2) $1 \cdot 10^{-5}$ M, (3) $5 \cdot 10^{-5}$ M, (4) $2 \cdot 10^{-4}$ M, (5) $1 \cdot 10^{-3}$ M.

obtained with plates 0.8-cm thick is shown in Figure 3. The data demonstrate that the reaction rate depends on the concentrations of both methyl viologen and sodium dithionite, which distinguishes the kinetics of the heterogeneous reaction from the kinetics observed in solution. Preliminary experiments with soluble enzymes have shown that the presence of excess sodium dithionite does not affect the reaction rate and that the role of sodium dithionite is limited to maintaining the constant concentration of methyl viologen by converting its oxidized form to the reduced one. With the heterogeneous reaction, diffusion of not only methyl violation but also sodium dithionite becomes important. So it is necessary to take into consideration the diffusion of two substrates. This problem is discussed below.

DISCUSSION

A Mathematical Model of a Heterogeneous Catalytic System Including an Intermediate Electron Donor

We consider a two-step catalytic reaction occurring in a plate (membrane) that contains an enzyme evenly distributed over its bulk. We

assume that constant substrate concentrations at the membrane surface are maintained in solution. Let the membrane first be saturated with the second substrate in the form S_2'. The substrate in the solid phase is assumed to be in equilibrium with the same substrate in solution. Then we introduce into the system excess substrate S_1. The substrate S_1 converts the form S_2' into S_2 in solution. The same transformation occurs as S_1 diffuses into the plate. We assume that the equilibrium distribution of the second substrate between the two phases does not shift on the replacement of S_2' with S_2, that is, that S_2' and S_2 have the same distribution coefficients. The proton concentration does not change during the reaction because of high buffer concentrations.

According to the two-step scheme (1), two reaction zones occur in the membrane (see Fig. 4). The first zone contains excess S_1 and therefore the S_2 form of substrate 2. The S_2' form produced in the second step undergoes instantaneous transformation to S_2 in the presence of S_1. The second zone contains the second substrate in the initial form S_2'. Under steady state conditions (the nonsteady state problem is not considered here), the diffusion flows of S_1 from the left-hand side and S_2' from the right-hand side compensate each other at the interface separating the two zones. The substrate S_2 formed at the interface diffuses into the second zone and undergoes consumption according to the second step of reaction (1).

The expression for the enzymatic reaction may be written

$$V([S_2]) = \frac{V_{max}[S_2]}{K_m + [S_2]}, \tag{2}$$

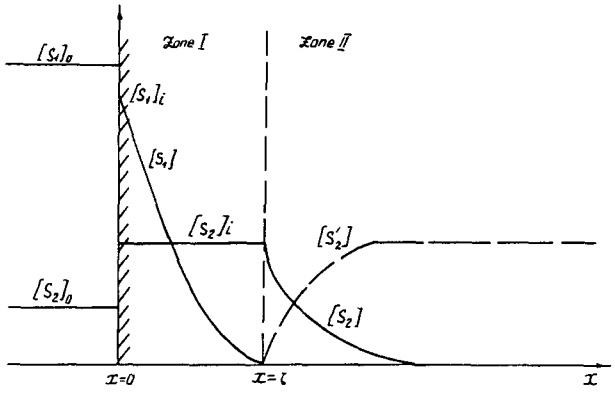

FIG. 4. A schematic representation of substrate concentration profiles in membranes containing immobilized enzymes under the conditions of two consequtive reactions.

where V is the local reaction rate (the rate of reduction of hydrogen ions); V_{max} the maximum reaction rate dependent on the concentration of the enzyme and proton concentration; $[S_2]$ the local concentration of the second substrate; K_m the Michaelis–Menten constant for immobilized hydrogenase. In the first zone the reaction rate is constant and equal to $V([S_2]_i)$ over the plate thickness where $[S_2]_i$ is the concentration of the second substrate which is in equilibrium with its concentration in solution $[S_2]_0$.

On the assumptions made the boundary value problem may be written as follows:

$$aD_1(d^2[S_1]/dx^2) = V([S_2]_i) \quad \text{if} \quad 0 < x < \zeta \tag{3}$$

$$[S_1] = 0 \qquad \zeta \leq x \leq l \tag{4}$$

$$[S_2] = [S_2]_i = P_2[S_2]_0 \qquad 0 \leq x \leq \zeta \tag{5}$$

$$D_2(d^2[S_2]/dx^2) = V([S_2]) \qquad \zeta < x < l \tag{6}$$

$$[S_1] = P_1[S_1]_0 \qquad x = 0 \tag{7}$$

$$aD_1(d[S_1]/dx) = D_2(d[S_2]/dx) \qquad x = \zeta \tag{8}$$

$$d[S_2]/dx = 0 \qquad x = l \tag{9}$$

where $[S_1]$ is the local concentration of S_1 in the membrane; $[S_1]_0$ and $[S_2]_0$ are the concentrations of the substrates in solution; D_1 and D_2 the diffusion coefficients; P_1 and P_2 the distribution coefficients for the substrates S_1 and S_2, respectively; x is the distance from the membrane surface; ζ the coordinate of the interface; l the coordinate of the symmetry plane of the membrane, or the membrane thickness if the membrane is accessible to solution on one side only. The local concentration $[S_2']$ is given by $[S_2]_i - [S_2]$. Condition (7) means that no accounting is made of external diffusion resistance.

The expression for the product (molecular hydrogen) flux including the stoichiometric coefficients has the form

$$j = -aD_1\sigma/2 \cdot d[S_1]/dx|_{x=0} = (\sigma/2)V([S_2]_i)\zeta + (\sigma/2)\int_{\zeta}^{l} V([S_2])\,dx \tag{10}$$

where σ is the plate surface area.

A particular case of the substrate S_1 diffusing through the whole plate thickness should be considered. The reaction then proceeds under purely kinetic control and

$$j = (\sigma l/2)V([S_2]_i) \tag{11}$$

The problem of the number of parameters that fully determine the behavior of the system is of importance. To solve this problem, we introduce dimensionless variables $\eta \equiv x/l$;

$$\theta \equiv [S_1]/P_1[S_1]_0; \qquad \theta_2 \equiv [S_2]/P_2[S_2]_0; \qquad \zeta^* = \zeta/l.$$

Equations (3)–(9) may then be rewritten in the form

$$d^2\theta_1/d\eta^2 = N_1/(N_2+1) \qquad \text{if} \quad 0<\eta<\zeta^* \tag{12}$$

$$\theta_1 = 0 \qquad \zeta^* \le \eta \le 1 \tag{13}$$

$$\theta_2 = 1 \qquad 0 \le \eta \le \zeta^* \tag{14}$$

$$d^2\theta_2/d\eta^2 = N_1\theta_2/N_3(N_2+\theta_2) \qquad \zeta^*<\eta<1 \tag{15}$$

$$\theta_1 = 1 \qquad \eta = 0 \tag{16}$$

$$d\theta_1/d\eta = N_3(d\theta_2/d\eta) \qquad \eta = \zeta^* \tag{17}$$

$$d\theta_2/d\eta = 0 \qquad \eta = 1 \tag{18}$$

where $N_1 \equiv (V_{max}l^2)/aP_1D_1[S_1]_0$, $N_2 \equiv K_m/P_2[S_2]_0$, $N_3 \equiv P_2D_2[S_2]_0/aP_1D_1[S_1]_0$ are dimensionless criterions. Equation (10) then becomes

$$j = \frac{aP_1D_1\sigma[S_1]_0}{2l} \cdot \frac{d\theta_1}{d\eta}\bigg|_{\eta=0} \tag{19}$$

The derivative $d\theta_1/d\eta$ ($\eta = 0$) depends on the dimensionless values N_1, N_2, and N_3. The flux from the plate thus depends on these three criterions and on the dimensional value $aP_1D_1\sigma[S_1]_0/l$. It follows that an experimental study of the product flux from the plate allows us to determine no more than four system parameters. For instance, an experimental study of j as depending on the experimental system parameters $[S_1]_0$, $[S_2]_0$, l and σ affords only four combinations of internal parameters entering the expressions for N_1, N_2, and N_3, namely V_{max} and the criterions K_m/P_2; aP_1D_1; P_2D_2.

General Solution

Using the transform $y_j = d\theta_j/d\eta$ where $j = 1, 2$, so that $d^2\theta_j/d\eta^2 = dy_j/d\eta = y_j \cdot dy_j/d\theta_j$, we may rewrite Eqs. (12) and (15) in the form

$$y_1\, dy_1 = [N_1/(N_2+1)]\, d\theta_1 \tag{20}$$

$$y_2\, dy_2 = [N_1\theta_2/N_3(N_2+\theta_2)]\, d\theta_2 \tag{21}$$

Integration of (20) from $\eta = 0$ to $\eta = \zeta^*$ yields

$$[(d\theta_1/d\eta)(\eta = 0)]^2 - [(d\theta_1/d\eta)(\eta = \zeta^*)]^2 = 2N_1/(N_2 + 1) \tag{22}$$

Taking into consideration (18) and (14), we obtain by integration of (21)

$$\frac{d\theta_2}{d\eta} = -\left[\frac{2N_1}{N_3}\left(\theta_2 - \theta_2(1) + N_2 \ln \frac{N_2 + \theta_2(1)}{N_2 + \theta_2}\right)\right]^{1/2} \tag{23}$$

$$\left[\frac{d\theta_2}{d\eta}(\eta = \zeta^*)\right]^2 = \frac{2N_1}{N_3}\left(1 - \theta_2(1) + N_2 \ln \frac{N_2 + \theta_2(1)}{N_2 + 1}\right) \tag{24}$$

Equations (22), (17), and (24) relate the product flux to the concentration $\theta_2(1)$.

In order to determine $\theta_2(1)$ and the interface coordinate ζ^*, equation (12) should be integrated while taking into consideration of (13) and (16)

$$\theta = A\eta^2 - [A\xi^* + (1/\zeta^*)]\eta + 1 \tag{25}$$

where $A \equiv N_1/2(N_2 + 1)$. The condition of conjugation (17), and (24) and (25) yield

$$\frac{1}{\zeta^*} - A\zeta^* = \left[2N_1N_3\left(1 - \theta_2(1) + N_2 \ln \frac{N_2 + \theta_2(1)}{N_2 + 1}\right)\right]^{1/2} \tag{26}$$

Taking into consideration (14) and integrating (23) from $\eta = \zeta^*$ to $\eta = 1$, we obtain .

$$1 - \zeta^* = \left(\frac{N_3}{2N_1}\right)^{1/2} \int_{\theta_2(1)}^{1} \{\theta_2 - \theta_2(1) + N_2 \ln [(N_2 + \theta_2(1))/(N_2 + \theta_2)]\}^{-1/2}\, d\theta_2 \tag{27}$$

The set (26), (27) determines the sought values ζ^* and $\theta_2(1)$.

The principal difficulty one encounters in the numerical solution of (26), (27) is the calculation of the integral entering the right-hand side of equation (27). With $\theta_2 = \theta_2(1)$, the integrand has a singularity. It is easy, however, to show that this improper integral converges.

Substitution

$$(N_2 + \theta_2)/[N_2 + \theta_2(1)] = 1 + u$$

transforms the integral entering the equation (27) to

$$I = [N_2 + \theta_2(1)] \int_0^c \{u[N_2 + \theta_2(1)] - N_2 \ln(1 + u)\}^{-1/2}\, du$$

where

$$c \equiv [1 - \theta_2(1)]/[N_2 + \theta_2(1)]$$

Using the Taylor formula we obtain

$$u[N_2+\theta_2(1)]-N_2\ln(1+u)=\theta_2(1)u+(au^2/2)-[au^3/3(1+2au)^3]$$

where $0<a<1$. Hence

$$\{u[N_2+\theta_2(1)]-N_2\ln(1+u)\}^{-1/2}=[\theta_2(1)u+(au^2/2)]^{-1/2}(1-\beta)^{-1/2}$$

where

$$\beta=au^3/3(1+au)^3[\theta_2(1)u+(au^2/2)]<\frac{2}{3}u$$

Repeated application of the Taylor formula yields

$$(1-\beta)^{-1/2}=1+[\beta/2(1-\gamma\beta)^{3/2}]$$

where $0<\gamma<1$.
Let u be equal to 10^{-3}. Then

$$\beta/2(1-\gamma\beta)^{3/2}<4\cdot 10^{-4}$$

The integral entering (27) may thus be represented as the sum $I=I_1+I_2$ where

$$I_1=\int_0^{u_0}\{u[N_2+\theta_2(1)]-N_2\ln(1+u)\}^{-1/2}\,du\approx\int_0^{u_0}[\theta_2(1)u+au^2/2]^{-1/2}\,du$$

$$=(2/N_2)^{1/2}\ln\left\{1+\frac{u_0a}{\theta_2(1)}+\left[\frac{u_0^2a^2}{[\theta_2(1)]^2}+2\frac{u_0a}{\theta_2(1)}\right]^{1/2}\right\} \tag{28}$$

$$I_2=\int_{u_0}^{c}\{u[N_2+\theta_2(1)]-N_2\ln(1+u)\}^{-1/2}\,du \tag{29}$$

With u_0 equal to 10^{-3}, the first integral may be calculated using the analytical expression (28) with an accuracy of 0.04%. The second integral may be calculated with any desired accuracy by the standard numerical methods.

Note that this calculation technique is also applicable with a one-substrate reaction occurring in a plate of finite thickness and following the Michaelis–Menten equation (19–22). The latter problem leads to equation (27) with $\zeta^*=0$.

Asymptotic Approximations

Plate of Infinite Thickness. With sufficiently large N_1, the concentration S_2 may be thought to reduce to zero in the region remote from the plate surface. That is, boundary condition (9) should be replaced with

$$[S_2]\longrightarrow 0 \quad \text{if} \quad x\longrightarrow\infty \tag{30}$$

The corresponding equation for the product flux may be obtained using equation (24) with $\theta_2(1)$ equal to 0:

$$j^2 = \frac{\sigma^2}{2} \cdot \frac{aP_1D_1V_{max}[S_2]_0}{K_m/P_2+[S_2]_0}[S_1]_0 + \frac{\sigma^2}{2}P_2D_2V_{max}\left\{[S_2]_0 + \frac{K_m}{P_2}\ln\frac{K_m/P_2}{K_m/P_2+[S_2]_0}\right\} \tag{31}$$

With $[S_1]_0$ equal to zero (31) becomes the known equation for a one-substrate reaction (19,23–24).

Step-Wise Reaction Front. Let N_3 approach zero. The concentration θ_2 profile in the vicinity of ζ^* should then be more sharp than the θ_1 profile [cf. condition (17)]. That means that the region of the main fall of θ_2 will be narrow in comparison with the first zone thickness. In this case the contribution from the integral on the right-hand side of equation (10) to the summary product yield will be only insignificant.

The problem may accordingly be simplified by neglecting the flux of S_1 at the interface, that is, by replacing the condition of conjugation (17) with

$$d\theta_1/d\eta = 0 \qquad \text{if} \qquad \eta = \zeta^* \tag{32}$$

The function $\theta_1(\eta)$ is then completely determined by equations (12), (13), (16), and (32).

The set of equations for the determination of θ_2,—(14), (15), and (18), then degenerates into a step-wise function

$$\theta_2(\eta) = \begin{cases} 1 & \text{if} \quad 0 \le \eta < \zeta^* \\ 0 & \text{if} \quad \zeta^* < \eta \le 1 \end{cases} \tag{33}$$

Accordingly, the reaction rate function undergoes a step-wise change from $V([S_2]_i)$ to 0 at ζ^*.

Equations (25) and (32) give

$$\zeta^* = 1/A^{1/2} \tag{34}$$

Hence, we find using the formula (10)

$$j = \frac{\sigma}{2}V([S_2]_i)l\zeta^* = \sigma\left[\frac{aP_1D_1V_{max}[S_1]_0}{2(1+K_m/P_2[S_2]_0)}\right]^{1/2} \tag{35}$$

Expression (35) is also easy to obtain from equations (19), (22), and (32).

Clearly, as A diminishes and ζ^* approaches unity, the stepwise model transforms naturally into a purely kinetic model (Eq. 11).

Equation (26) provides a strict definition of the sufficient conditions for the applicability of the stepwise model. We obtain from this equation

$$\zeta^* = -\frac{B\varepsilon}{2A} + \left(\frac{B^2\varepsilon^2}{4A^2} + \frac{1}{A}\right)^{1/2} \tag{36}$$

where

$$B \equiv (2N_1N_3)^{1/2}; \qquad \varepsilon \equiv \{1-\theta_2(1)+N_2\ln[(N_2+\theta_2(1))/(N_2+1)]\}^{1/2} \leq 1.$$

Clearly, with $B^2/4A \ll 1$, the equality (36) becomes (34). The sufficient condition for the applicability of the stepwise model may thus be written in the form

$$N_3(N_2+1) \ll 1 \tag{37}$$

Calculation of Model Parameters

Estimation of the left-hand side of inequality (37) using the K_m for the native enzyme has shown that most experimental points obtained with membranes 0.8-cm thick satisfy the requirement (37). The calculation of model parameters has therefore been carried out at the level of the step-wise reaction front approximation. Two points only were excluded that corresponded to $[S_2]_0/[S_1]_0 \sim 1$.

In terms of the stepwise model three parameters entering equations (35) and (11) only can be determined. These are V_{max}, $K_m^* = K_m/P_2$, and $D^* = aP_1D_1$.

The algorithm used to solve the inverse problem numerically was as follows. Let there be n experimental flux values $j_{exp}(i)$, where $i = 1,2,\ldots,n$, corresponding to various initial concentrations $[S_1]_0(i)$ and $[S_2]_0(i)$ and to given values of l, 0.8 cm, and σ, 10 cm^2. Using equation (34) we calculate $\zeta^*(i)$ with V_{max}, K_m^*, and D^* as arguments for each i value. Depending on whether the inequality $\zeta^* \leq 1$ or $\zeta^* \geq 1$ is satisfied, the expressions (35) and (11) are used to calculate the product flux values $j(i)$ for each set of parameters V_{max}, K_m^*, and D^*. The solution of the inverse problem reduces to minimization of the function

$$Q(V_{max}, K_m^*, D^*) = \left\{\sum_{i=1}^{n}\left[1-\frac{j(i)}{j_{exp}(i)}\right]^2\right\}^{1/2}$$

This problem was solved by using the algorithm for multidimensional nonlocal random searching (25). The calculations were performed on a BESM-6 computer.

The parameter values corresponding to the minimal quality criterion value $Q = 0.909$ were $V_{max} = 2.4\cdot10^{-9}$ g-equiv H/cm^3·sec; $K_m/P_2 = 1.2\cdot10^{-5}$ M; $aP_1D_1 = 5\cdot10^{-7}$ cm^2/sec. Table 1 summarizes the experimental data and the hydrogen flux values calculated using the obtained parameter values. The agreement should be regarded as satisfactory if one considers that the percentage of active and accessible for the reagents immobilized enzyme and the properties of the gel matrix varied to a certain extent from

one experiment to another. Table 1 also includes the values of the interface coordinate calculated for each particular case. It is seen that sodium dithionite only penetrates through the whole plate thickness when its concentration exceeds that of methyl viologen by more than four orders of magnitude.

TABLE 1. **The Experimental and Calculated Hydrogen Flux Values and the Values of the Interface Coordinate for a Membrane 0.8 cm Thick**

$[S_2]_0$, M	$[S_1]_0$, M	j_{exp} (mol/sec) $\times 10^{10}$	j_{calc} (mol/sec) $\times 10^{10}$	ζ, cm
$5.0 \cdot 10^{-7}$	$4.2 \cdot 10^{-5}$	$2.4 \cdot 10^{-2}$	$3.2 \cdot 10^{-2}$	0.065
$5.0 \cdot 10^{-7}$	$1.6 \cdot 10^{-3}$	0.30	0.20	0.40
$5.0 \cdot 10^{-7}$	$4.2 \cdot 10^{-3}$	0.41	0.32	0.65
$5.0 \cdot 10^{-7}$	$1.1 \cdot 10^{-2}$	0.44	0.39	0.80[a]
$8.1 \cdot 10^{-7}$	$4.2 \cdot 10^{-3}$	0.50	0.40	0.52
$1.5 \cdot 10^{-6}$	$4.2 \cdot 10^{-3}$	0.60	0.55	0.39
$3.7 \cdot 10^{-6}$	$4.2 \cdot 10^{-3}$	0.75	0.80	0.27
$7.6 \cdot 10^{-6}$	$4.2 \cdot 10^{-3}$	1.0	1.0	0.20
$1.0 \cdot 10^{-5}$	$3.5 \cdot 10^{-4}$	0.36	0.32	0.056
$1.0 \cdot 10^{-5}$	$5.7 \cdot 10^{-4}$	0.40	0.40	0.071
$1.0 \cdot 10^{-5}$	$9.5 \cdot 10^{-4}$	0.65	0.50	0.092
$1.0 \cdot 10^{-5}$	$1.6 \cdot 10^{-3}$	0.55	0.65	0.12
$1.0 \cdot 10^{-5}$	$2.0 \cdot 10^{-3}$	0.55	0.75	0.13
$1.0 \cdot 10^{-5}$	$3.2 \cdot 10^{-3}$	1.0	0.95	0.17
$1.0 \cdot 10^{-5}$	$4.2 \cdot 10^{-3}$	1.2	1.1	0.19
$1.0 \cdot 10^{-5}$	$1.1 \cdot 10^{-2}$	1.4	1.7	0.31
$1.5 \cdot 10^{-5}$	$4.2 \cdot 10^{-3}$	1.3	1.2	0.17
$3.7 \cdot 10^{-5}$	$4.2 \cdot 10^{-3}$	1.6	1.4	0.15
$7.6 \cdot 10^{-5}$	$4.2 \cdot 10^{-3}$	1.7	1.5	0.14
$1.5 \cdot 10^{-4}$	$4.2 \cdot 10^{-3}$	1.6	1.6	0.14
$2.0 \cdot 10^{-4}$	$1.7 \cdot 10^{-3}$	1.2	1.0	0.084
$2.0 \cdot 10^{-4}$	$1.1 \cdot 10^{-2}$	2.6	2.5	0.21
$2.0 \cdot 10^{-4}$	$1.4 \cdot 10^{-2}$	2.5	2.9	0.25
$3.7 \cdot 10^{-4}$	$4.2 \cdot 10^{-3}$	1.6	1.6	0.13
$7.6 \cdot 10^{-4}$	$4.2 \cdot 10^{-3}$	1.7	1.6	0.13
$1.0 \cdot 10^{-3}$	$6.8 \cdot 10^{-4}$	0.70	—	—
$1.0 \cdot 10^{-3}$	$1.4 \cdot 10^{-3}$	0.90	—	—
$1.0 \cdot 10^{-3}$	$1.8 \cdot 10^{-3}$	0.95	1.1	0.087
$1.0 \cdot 10^{-3}$	$3.0 \cdot 10^{-3}$	1.7	1.4	0.11
$1.0 \cdot 10^{-3}$	$4.0 \cdot 10^{-3}$	1.7	1.6	0.13
$1.0 \cdot 10^{-3}$	$1.0 \cdot 10^{-2}$	2.6	2.5	0.20

[a] Sodium dithionite penetrates through the whole plate thickness.

Independent Testing of the Model

Measurement of Reaction Rates in Thin Plates. As seen from Table 1, most experimental data obtained with plates 0.8-cm thick correspond to well below saturation conditions, $\zeta^* \ll 1$ (although complete and next to complete saturation in several experiments of the series is essential to simultaneous determination of aP_1D_1 and V_{max}). A series of kinetic measurements was made with thinner plates, of a 0.18-cm thickness, under the conditions when sodium dithionite penetrated through the whole plate thickness ($[S_1]_0 \geq 10^{-2}$ M). These data provide an independent determination of V_{max} and K_m/P_2 under purely kinetic control. The parameter values calculated using equation (11) are $V_{max} = (3.2 \pm 0.6) \cdot 10^{-9}$ g-equiv $H/cm^3 \cdot sec$, and $K_m/P_2 = 0.9 \cdot 10^{-5}$M, which agree satisfactorily with the results of the first series of measurements.

Measurement of Displacement of the Colored Reaction Zone Boundary. Direct determination of the distribution coefficient and diffusion coefficient in gel for sodium dithionite which undergoes oxidation with air oxygen exceedingly readily is a complex experimental task. A special technique was applied to determine the parameter aP_1D_1 independently. This was done by visual monitoring of displacement of the first reaction step zone front during diffusion of sodium dithionite in an acrylamide gel column. For this purpose, the gel column was saturated with the oxidized form of methyl viologen S_2'. Displacement of the reaction front was followed by propagation of a blue coloration characteristic of the reduced form of methyl viologen S_2 (the form S_2' is colorless). In essence, these experiments only differed from the main kinetic experiments in that no enzyme was introduced into acrylamide gel and therefore the second reaction step did not take place.

The corresponding nonsteady-state diffusion problem was solved in (26). The position of the interface separating the zones of two reacting substance S_1 and S_2' satisfies equation

$$\zeta = 2(\mu t)^{1/2} \tag{38}$$

where t is time and μ is the root of the transcendental equation

$$\frac{aP_1[S_1]_0(D_1)^{1/2}}{\operatorname{erf}(\mu/D_1)^{1/2}} \exp\left(-\frac{\mu}{D_1}\right) = \frac{P_2[S_2]_0(D_2)^{1/2}}{1-\operatorname{erf}(\mu/D_2)^{1/2}} \exp\left(-\frac{\mu}{D_2}\right) \tag{39}$$

The constant μ is easy to determine experimentally.

Equation (39) may be rewritten in the form

$$1 = \operatorname{erf}\left(\frac{\mu}{D_2}\right)^{1/2} + \frac{P_2[S_2]_0}{aP_1[S_1]_0}\left(\frac{D_2}{D_1}\right)^{1/2} \operatorname{erf}\left(\frac{\mu}{D_1}\right) \exp\left(\frac{\mu}{D_1} - \frac{\mu}{D_2}\right) \tag{40}$$

Under the condition $N_3 \ll 1$ and with D_1 and D_2 having not very different

values, equation (40) gives $\mathrm{erf}(\mu/D_i) \approx 1$ where $i = 1,2$. Expansion of the function $\mathrm{erf}(\mu/D_2)^{1/2}$ entering the right-hand side of equation (39) into an asymptotic series for large argument values transforms (39) into

$$\frac{\exp(-\mu/D_1)}{(\mu/D_1)^{1/2}} = \pi^{1/2}\frac{P_2[S_2]_0}{aP_1[S_1]_0} \tag{41}$$

Equation (41) corresponds to the approximation of stepwise variation of the concentrations S_2' and S_2. This equation may be used to find D_1 and aP_1/P_2 simultaneously if the μ values are determined for at least two different concentration ratios $[S_2]_0/[S_1]_0$. In this case

$$D_1 = \frac{\mu_2 - \mu_1}{\ln[(\mu_1)^{1/2}([S_2]_0/[S_1]_0)_1/(\mu_2)^{1/2}([S_2]_0/[S_1]_0)_2]} \tag{42}$$

The experimental data are given in Figure 5. The presence of a well-defined boundary that undergoes displacement with time is in itself a direct substantiation of the stepwise reaction front model suggested above.

It should however be noted that the boundary becomes diffuse at sufficiently large distances from the plate surface (of about 2 to 3 cm). That means that diffusion penetration of S_2 into the region $x > \zeta$ becomes important (see Fig. 4); under these conditions the position of the colored boundary cannot be determined accurately, and this boundary does not correspond strictly to coordinate ζ.

The application of this technique yielded the following parameter values: $D_1 = (1.5 \pm 0.8) \cdot 10^{-6}$ cm^2/sec; $aP_1/P_2 = 0.4 \pm 0.2$. The special equilibrium experiments were carried out to determine the distribution

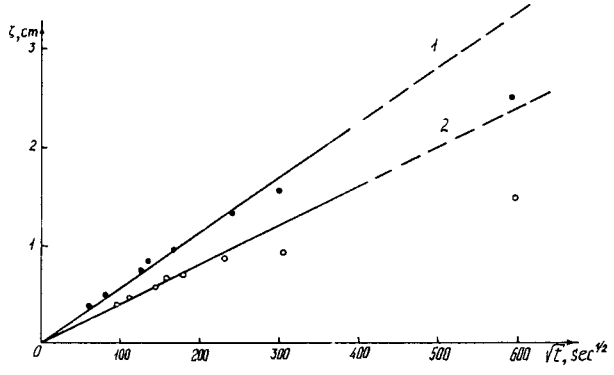

FIG. 5. Experimental data on shifting of the coloured reaction zone boundary in a polyacrylamide gel column. (1) $[S_2]_0/[S_1]_0 = 1.5 \cdot 10^{-3}$ (2) $[S_2]_0/[S_1]_0 = 1.5 \cdot 10^{-2}$.

coefficient for methyl viologen, $P_2 = 2.0 \pm 1.0$. Hence $aP_1D_1 = (1.2 \pm 0.9) \cdot 10^{-6}$ cm^2/sec which agrees with the results of the kinetic measurements to within measurement error.

ACKNOWLEDGMENTS

The authors wish to express their thanks to Prof. I. V. Berezin for interest in this work and for detailed discussions of the results obtained.

REFERENCES

1. GREGORY, D. P. (1973) Sci. American 228 : 13.
2. WINSCHE, W. E., HOFFMAN, K. C., and SALZANO, F. J. (1973) Science 180 : 1325.
3. QADRI, S. M. H., and HOARE, D. S. (1968) J. Bacteriol. 95 : 2344.
4. SCHLEGEL, H. G., and EBERHARDT, U. (1972) Adv. Microbiol. Physiol. 7 : 205.
5. MORTENSON, L. E., and CHEN, J.-S. (1974) *In* Microbial Iron Metabolism, NEILANDS, J. B. (ed.), Academic Press, New York, p. 231.
6. KONDRAT'EVA, E. N., and GOGOTOV, I. N. (1976) Izv. Akad. Nauk SSR, Ser. Biol., No. 1, 69.
7. BENEMANN, J. R., BERENSON, J. A., KAPLAN, N. O., and KAMEN, M. D. (1973), Proc. Natl. Acad. Sci. US 70 : 2317.
8. BEREZIN, I. V., VARFOLOMEEV, S. D., and ZAITSEV, S. V. (1976) Dokl. Akad. Nauk SSR 229 : 94.
9. BEREZIN, I. V., and VARFOLOMEEV, S. D. (1976) Geliotekhnika 3 : 60.
10. BEREZIN, I. V., VARFOLOMEEV, S. D., YAROPOLOV, A. I., TARASEVICH, M. R., and BOGDANOVSKAYA, V. A. (1976) Dokl. Akad. Nauk SSSR 225 : 105.
11. VARFOLOMEEV, S. D., YAROPOLOV, A. I., BEREZIN, I. V., TARASEVICH, M. R., and BOGDANOVSKAYA, V. A., (1977) Bioelectrochem. Bioenergetics 4 : 314.
12. BEREZIN, I. V., VARFOLOMEEV, S. D., TOAI, CH. -D., GOGOTOV, I. N., and ZORIN, N. A. (1975) Dokl. Akad. Nauk SSSR 220 : 237.
13. TOAI, CH. -D., VARFOLOMEEV, S. D., GOGOTOV, I. N., and BEREZIN, I. V. (1976) Mol. Biol. 10 : 452.
14. NGO, T. T., and LAIDLER, K. J. (1975) Biochem. Biophys. Acta 377 : 303.
15. ELOFSON, R. M., and EDSBERG, R. L. (1957) Can. J. Chem. 35 : 646.
16. VARFOLOMEEV, S. D., BACHURIN, S. O., TOAI, CH-D., and GOGOTOV, I. N. (1978) Mol. Biol. (USSR) 12 : 63.
17. LUR'E, YU. YU. (1971) Spravochnik po analiticheskoi Khimii (Handbook on analytical Chemistry), Moscow, Khimiya Publ.
18. LAMBETH, D. O., and PALMER, G. (1973) J. Biol. Chem. 248 : 17, 6095.
19. ROBERTS, G. W., and SATTERFIELD, G. N. (1965) Ind. Eng. Chem. Fundamentals 4 : 288.
20. CHU, C., and HOUGEN, O. A. (1962) Chem. Eng. Sci. 17 : 167.
21. SCHNEIDER, P., and MITSCHKA, P. (1965) Collection Czechoslov. Chem. Commun. 30 : 146.
22. SUNDAAM, P. V., TWEEDALE, A., and LAIDLER, K. J. (1970) Can. J. Chem. 48 : 1498.
23. BISCHOFF, K. B. (1965) AIChE J. 11 : 351.

24. HAMILTON, B. K., GARDNER, C. R., and COLTON, C. K., (1974) AIChE J. 20 : 3, 503.
25. MITROFANOV, V. B. (1974) Ob odnom Algoritme eluchainogo Poiska (On one Algorithm of Random Search), Moscow, Institute of Applied Mathematics of the USSR Academy of Sciences, Preprint No. 118.
26. ASTARITA, G. (1967) Mass Transfer with Chemical Reaction, Elsevier Publishing Company, Amsterdam.